Analytical Methods

PAPER

View Article Online
View Journal | View Issue

Cite this: *Anal. Methods*, 2017, **9**, 3255

Bright red fluorescent conjugated polymer nanoparticles with dibenzopyran as electron donor for cell imaging†

Mengyue Fan,‡[a] Yuanyuan Zhou,‡[b] Yijing Guo,[b] Jinsheng Song *[b] and Xinrui Duan *[a]

Received 5th March 2017
Accepted 10th May 2017

DOI: 10.1039/c7ay00585g

rsc.li/methods

Fluorescent conjugated polymers (CPs) have been successfully used to make conjugated polymer nanoparticles (CPNs) for cellular imaging, bio-orthogonal labeling, and *in vivo* tumor targeting, since CPNs have superior bright fluorescent emission and photostability. However, the preparation of red fluorescent CPNs with reasonably high quantum yield (QY) is still very challenging. We have synthesized bright red fluorescence CPNs based on a conjugated polymer that contains an annulated pyran ring and branched alkoxy chains, which have helped to reduce close packing in the solid phase. We examined the impact of the molecular weight of CPs on the QYs of CPNs. QY as high as 51.8–36.8% was observed in all CPNs with normally used CPs, with a surfactant mass ratio of 1 : 2. Our CPNs provided intense and stable fluorescence which could be traced through several generations in cell imaging, indicating the considerable photostability and biocompatibility of our CPNs.

Conjugated polymers (CPs) have large π-conjugated backbones and a delocalized electronic structure, allowing excited energy to move along the polymer backbone through overlaps in the π-electron clouds by hopping, tunneling, and related mechanisms.[1] Due to their excellent fluorescent characteristics, fluorescent CPs have been widely used in bioimaging and biosensing.[2] Conjugated polymer nanoparticles (CPNs) maintain the excellent fluorescence properties of CPs with the additional benefits of easy surface functionalization and minimal cytotoxicity.[3] Indeed, CPNs have a greater photostability and fluorescence brightness than small molecule organic dyes and inorganic semiconductor quantum dots (QDs), and CPNs do not contain heavy metal ions that may leak from fluorescent QDs and cause potential cytotoxicity.[4]

Fluorescent CPs, such as poly[(9,9-dioctylfluorenyl-2,7-diyl)-*alt*-1,4-benzo-(2,1,3)-thiadiazole] (PFBT) and poly(*p*-phenylenevinylene) (PPV), have been successfully used to make CPNs for cellular imaging, bio-orthogonal labeling, and *in vivo* tumor targeting.[5] However, the preparation of red fluorescent CPNs with a reasonable high quantum yield (QY) is still very challenging.[6] Red CPNs from a mixture of CPs with red small molecule organic dyes have been reported, but the unique optical properties of CPs are unavoidably compromised.[7] Usually, the rigid and flat extended π-conjugated skeletons of red fluorescent CPs exhibit serious self-quenching after condensation into nanoparticles.[8] By using an unusually low mass ratio of CPs and an amphiphilic polymer, CPs can be dispersed into each nanoparticle as single polymer chain to prevent the aggregation-induced fluorescence quenching.[9] Theoretically, nanoparticles with a higher packing capacity of CPs would have brighter fluorescence and higher photostability. To reduce the impact of the aggregation of CPs in nanoparticles, introduction of bulky pendants in the backbone or onto the side chain of CPs[10] and installation of alkyl chains on the comonomer have been used to increase the QY of CPNs.[11] After carefully examining these CPNs systems, it is easy to infer that fluorene and benzothiadiazole were the general building blocks in these red CPs syntheses. Recently, we have developed a new electron donating building block dibenzopyran (DBP), which possesses an annulated pyran ring in between the two benzene rings.[12] Our previous report indicates that the annulated pyran ring and the branched alkoxy chains are valuable in reducing the close packing in the solid phase. Thus, we propose that a similar design would also help to generate bright red fluorescent CPNs.

The red fluorescent **PDBPTBT-2** was synthesized *via* the Suzuki polycondensation of DBP and the branched alkoxy-chain-substituted benzothiadiazide.[12] Different portions with varied molecular weights were separated *via* Soxhlet extraction by acetone, hexane and dichloromethane, which are simplified

[a]*Key Laboratory of Analytical Chemistry for Life Science of Shaanxi Province, School of Chemistry and Chemical Engineering, Shaanxi Normal University, Xi'an, Shaanxi, 710119, P. R. China. E-mail: duanxr@snnu.edu.cn*

[b]*Engineering Research Center for Nanomaterials, Henan University, Kaifeng, Henan, 475004, P. R. China. E-mail: songjs@henu.edu.cn*

† Electronic supplementary information (ESI) available. See DOI: 10.1039/c7ay00585g

‡ These authors contribute equally to this work.

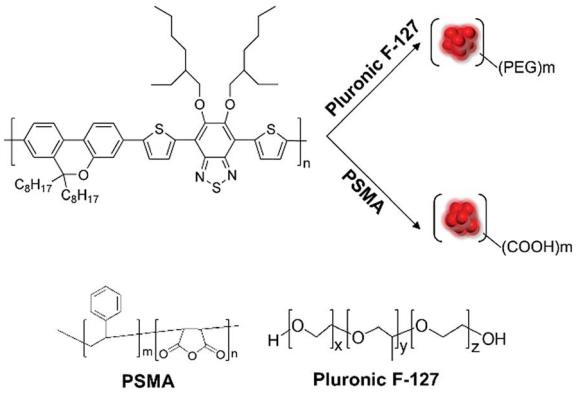

Scheme 1 Procedures for the preparation of water-soluble PDBPTBT-2 nanoparticles.

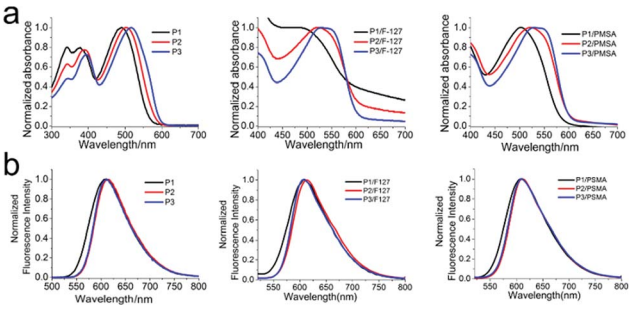

Fig. 1 (a) UV-visible spectra of PDBPTBT-2 in THF and PDBPTBT-2 NP series in aqueous solution, respectively. (b) Fluorescence spectra of PDBPTBT-2 in THF and PDBPTBT-2 NP series in aqueous solution, respectively. The excitation wavelength is 490 nm.

as **P-1**, **P-2** and **P-3**, respectively. The CP shows substantial absorptivity and efficient deep-red emission in an organic solvent. As shown in Scheme 1, we prepared our CPNs by rapid precipitation of **PDBPTBT-2** with two commonly used amphiphilic polymers, nonionic surfactant plutonic-F127 or poly(styrene-*co*-maleic anhydride) (PSMA), in the CPN synthesis. We examined the impact of the molecular weight of the CPs on the QYs of the CPNs. Due to the brightness and the long emission wavelength, these CPNs were subjected for cell imaging for 1 week. The CPNs are relatively stable for months without aggregation.

Red-emitting **PDBPTBT-2** was prepared according to the previously reported method.[12] Since the molecular weight of the CP has an important impact on the photophysical properties of the resulting fluorescent nanoparticles, **PDBPTBT-2** with different molecular weights (**P1–P3**) was prepared, with detailed information provided in Table S1.† Scheme 1 illustrates the procedures for the preparation of water-soluble CPNs. CPNs were prepared by a simple re-precipitation method. A tetrahydrofuran (THF) solution of CP with Pluronic F-127 (F-127) or poly(styrene-*co*-maleic anhydride) (PSMA) was quickly injected into water under sonication. Later, THF was removed by rotoevaporation to allow formation of the CPNs in an aqueous environment. As we observed in Scheme 1, F-127 does not have any chromophore or conjugated structure that would interfere with the measurement of the photophysical properties of the resulting CPNs. On the other hand, PSMA provided a functional group (–COOH) on the surface of the CPNs and created higher packing capacity of CPs. High packing capacity would help increase the brightness and photostability of single fluorescent nanoparticles. Both F-127 and PSMA are commonly used for the preparation of CPNs. This approach is very easy to handle and has good reproducibility. The resulting CPNs were quite stable, and no precipitate or aggregation were observed several months after preparation.

Ultraviolet-visible (UV-vis) absorption spectra of polymers **PDBPTBT-2** in THF solutions and CPNs in aqueous solution are shown in Fig. 1a, and data are listed in Table 1. The polymer and the CPNs present an absorption ranging from 300 to 600 nm, with two peaks located at around 550 nm (Band I) and 400 nm (Band II), respectively, which covers the wavelength of common exciting laser sources (*e.g.*, 405 nm, 488 nm, 535 nm, 559 nm *etc.*) for fluorescence microscopy as other CPs. Absorbance maxima appear at 490 nm, 500 nm, and 515 nm for **P-1** to **P-3** in THF, respectively. The absorbance maximum shifted slightly toward longer wavelength with increasing molecular weight of the polymer. All emission maxima of **P-1** to **P-3** appear at a wavelength around 610 nm (Fig. 1b). Like absorption spectra, a slight red-shift was observed with increasing molecular weight of the polymer. F-127 and PSMA both have hydrophobic and hydrophilic parts in their polymer chains. Under an aqueous environment, hydrophobic CPs are packed into their hydrophobic core, leaving the hydrophilic parts of the polymers facing the water. Since CPs remain well dispersed in a hydrophobic environment in the nanoparticle, the photophysical properties should be preserved very well. As we expected, all emission maxima of CPNs in water appear at a wavelength of around 610 nm, which is consistent with the emission of **PDBPTBT-2** in THF. Although the absorption spectra of **P-2** and **P-3** formed with nanoparticles (with Pluronic F-127 and PSMA) showed slightly red-shifted absorbance peaks, this might be due to the π–π stacking in the hydrophobic core of the nanoparticles. The QY of CPs in THF are around 70% (**P-1**: 70.6%; **P-2**: 71.4%; **P-3** 72.1%). In contrast, the QY of **P-1**, **P-2**, **P-3** in solid films are 40%, 28.8%, and 10.3%, respectively (Table S2†), since fluorescence quenching is often observed in solid films due to aggregation of the CPs, and is more significant as the molecular weight of the CPs increases. From Table 1, we can see that the QYs of the CPNs are higher than those in the solid film, but lower than the QYs in solution. This may also due to the stacking of multiple polymer chains in the single nanoparticles. However, the emission intensity of the fluorescence not only depends on the QY but also on the molar extinction coefficient of the CPNs. The fluorescence brightness can be estimated by multiplying the molar extinction coefficient with QY.[12] As can be seen in Table 1, **P-3**-based CPNs have the greatest brightness among the three CPs, with the **P-3**/PSMA being the brightest CPNs. In fact, **P-3**-based CPNs are nearly 10 times brighter than various organic dyes, and are comparable with QDs.[11]

The size of the NPs greatly affects its biomedical applications. For example, the size of NPs should be <200 nm for cell

Table 1 Photophysical properties of fluorescent nanoparticle in aqueous solution

	λ_{abs} (nm)	λ_{em} (nm)	Molar extinction coefficient (ε, M^{-1} cm^{-1})	Quantum yield (φ, %)	Brightness ($\varepsilon \times \varphi$, M^{-1} cm^{-1})
P-1/F127	490	605	1.2×10^4	51.8	6.0×10^5
P-2/F127	520	610	2.1×10^5	49.1	1.0×10^7
P-3/F127	540	607	1.0×10^6	37.4	3.7×10^7
P-1/PSMA	505	600	2.3×10^4	51.5	1.2×10^6
P-2/PSMA	520	605	2.2×10^5	50.8	1.1×10^7
P-3/PSMA	540	605	1.1×10^6	36.8	4.0×10^7

imaging *in vitro* and in the range 10–100 nm for efficient *in vivo* imaging. Hydrodynamic diameters of all CPNs were measured by dynamic light scattering, and results are shown in Fig. 2. As the molecular weight of the polymer increases, the size of the resulting NPs also increases. The particle sizes were further confirmed by transmission electron microscopy images (Fig. S1†). All nanoparticle sizes fell within the range 10–100 nm; thus, the sizes of all our CPNs are suitable for *in vivo* and *in vitro* imaging applications.[3]

To demonstrate the applicability of CPNs for biological imaging, we attempted to apply them to the long-term tracking of mammalian cells. To further increase the opportunity of CPNs to be retained inside cells, we modified our brightest CPNs (namely, **P-3**/PSMA) with ethyl 4-aminobutyrate hydrochloride *via* 1-ethyl-3-(3-dimethylaminopropyl)carbodiimide (EDC)-catalyzed coupling for cellular imaging (Scheme 2). The introduction of an ester group on the surface of the CPNs makes the particles more hydrophobic and should increase their non-specific binding onto the cellular membrane. Once the nanoparticle entered the cell, non-specific esterase would digest the esters into carboxylic acids, rendering the nanoparticles more hydrophilic and likely to be retained inside the cell.

To investigate results of the conjugation, we measured the ζ potential of all modified CPNs (Table 2). After conjugating different proportions of 4-aminobutyrate hydrochloride and glycine into the particle surface, the ζ potential significantly decreased from −43.61 (0% 4-aminobutyrate hydrochloride, 100% glycine) to −38.92 (50% glycine, 50% 4-aminobutyrate hydrochloride). The ζ potential of 10% 4-aminobutyrate (90% glycine)-modified nanoparticle differed slightly from that of P3/PSMA-50. Interestingly, when 100% 4-aminobutyrate hydrochloride was used, the resulting CPNs had a similar ζ potential

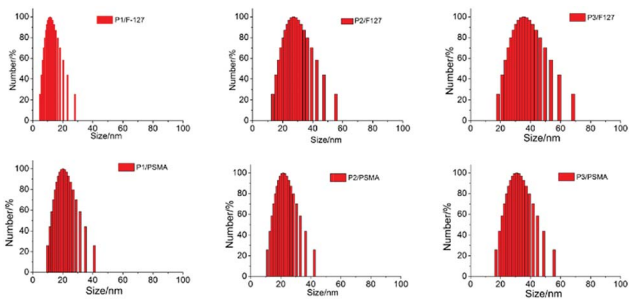

Fig. 2 Particles size of PDBPTBT NP series in aqueous solution by dynamic light scattering.

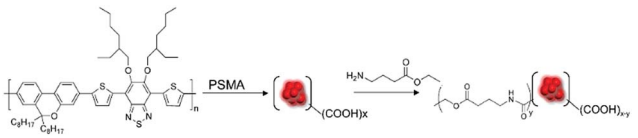

Scheme 2 Procedures for surface modification of CPNs with esters.

as P3/PSMA-10, which may be due to the hydrophobicity of the butyrate group which induced instability in the nanoparticles. Only the CPNs with a reasonable surface modification percentage could survive and remain in the aqueous solution.

Fig. 3 shows the laser confocal microscopy images of HCT-116 cells with various modified P3/PSMA at different time points. The CPNs were introduced into cells *via* 4 hour loading, and washed out after loading. Cells were passaged at Day 2, Day 4, Day 6, Day 8, and Day 10 with a ratio of 1 : 3. This means that cell proliferation would dilute the CPN concentration inside the cells three times after each passaging (48 hours). We were able to observe bright red fluorescence after the initial 4 hour loading. Merged images show the fluorescence signal of CPNs overlapping with the HCT-116 cells (Brightfield). Furthermore, the blank sample did not have a noticeable fluorescence emission signal under the same imaging conditions as the samples. These results indicate that our CPNs have a highly specific and effective cell staining ability. The fluorescence intensities of the images decrease as the dilution proceeds. Even after three passages (6 days), the fluorescence was still clearly observed. From a comparison of the relative fluorescence intensities of all CPNs with dilution curves (theoretical relative fluorescence intensities curve calculated based on cell passaging), we can see that the relative fluorescence intensities are higher than the theoretical relative fluorescence intensities. Thus, our functionalized CPNs provided intense and stable fluorescence that could be traced through several generations, indicating the considerable photostability and biocompatibility of our CPNs.

Table 2 Zeta potential of surface modified CPNs

	Zeta potential (mv)
P-3/PSMA-0	−43.61
P-3/PSMA-10	−40.91
P-3/PSMA-50	−38.92
P-3/PSMA-100	−40.27

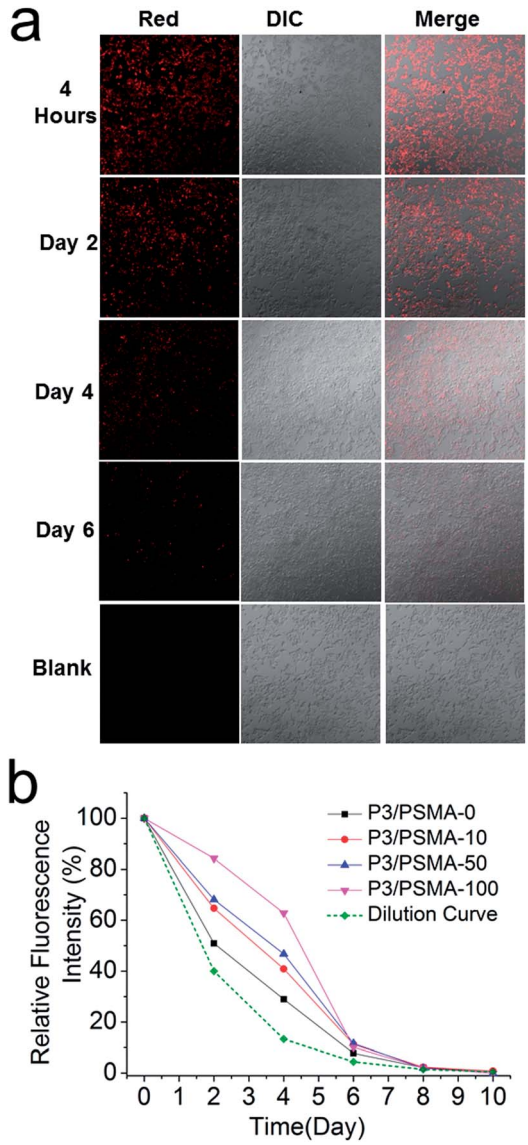

Fig. 3 (a) Laser confocal microscopy images of P3/PSMA-50 stained HCT-116 cells at 4 hours, 3 days, and 6 days, respectively; (b) relative average fluorescence intensity from images. The excitation wavelength is 559 nm. Cells were passaged at the ratio of 1 : 3 at Day 2, Day 4, Day 6, Day 8, Day 10. The dilution curve was calculated based on cell passaging ratio.

Furthermore, modified CPNs showed significantly slower decay in fluorescence intensities (Fig. 3b), which means that surface modification with esters further increased the CPN fluorescence in the cells.

Conclusions

In this paper, we have synthesized a bright red fluorescence CPN-based conjugated polymer that contains an annulated pyran ring and branched alkoxy chains. QY as high as 51.8–36.8% was observed in all CPNs with normally used CPs, with a surfactant mass ratio of 1 : 2. Due to the brightness and the red fluorescence emission, these CPNs were subjected to cell imaging for 1 week. Our functionalized CPNs provided intense and stable fluorescence that can be traced through several generations, indicating the considerable photostability and biocompatibility of our CPNs. Our molecular design of CPs provides a new approach to the preparation of bright CPNs with a high QY for biomedical imaging applications.

Acknowledgements

We are grateful to the National Natural Science Foundation of China (Grant No. 21675108, 21305083, 21404031, U1204212), and Fundamental Research Funds for the Central Universities (Grant No. GK201603028) for financial support.

Notes and references

1 (*a*) T. M. Swager, *Acc. Chem. Res.*, 1998, **31**, 201–207; (*b*) D. T. McQuade, A. E. Pullen and T. M. Swager, *Chem. Rev.*, 2000, **100**, 2537–2574.

2 (*a*) C. Zhu, L. Liu, Q. Yang, F. Lv and S. Wang, *Chem. Rev.*, 2012, **112**, 4687–4735; (*b*) X. Duan, L. Liu, F. Feng and S. Wang, *Acc. Chem. Res.*, 2010, **43**, 260–270; (*c*) K. Y. Pu and B. Liu, *Biosens. Bioelectron.*, 2009, **24**, 1067–1073.

3 (*a*) H. Peng and D. T. Chiu, *Chem. Soc. Rev.*, 2015, **44**, 4699; (*b*) J. Pecher and S. Mecking, *Chem. Rev.*, 2010, **110**, 6260–6279; (*c*) D. Tuncel and H. V. Demir, *Nanoscale*, 2010, **2**, 484–494; (*d*) H. Jiang, P. Taranekar, R. Reynolds and K. S. Schanze, *Angew. Chem., Int. Ed.*, 2009, **48**, 4300–4316; (*e*) K. Li, K. Y. Pu, L. P. Cai and B. Liu, *Chem. Mater.*, 2011, **23**, 2113–2119; (*f*) F. M. Kievit and M. Q. Zhang, *Adv. Mater.*, 2011, **23**, H217–H247.

4 (*a*) C. Wu and D. T. Chiu, *Angew. Chem., Int. Ed.*, 2013, **52**, 3086–3109; (*b*) V. N. Kilin, H. Anton, N. Anton, E. Steed, J. Vermot, T. E. Vandamme, Y. Mely and A. S. Klymchenko, *Biomaterials*, 2014, **35**, 4950–4957.

5 (*a*) K. Li and B. Liu, *Chem. Soc. Rev.*, 2014, **43**, 6570; (*b*) P. K. Kandel, L. P. Fernando, P. C. Ackroyd and K. A. Christensen, *Nanoscale*, 2011, **3**, 1037–1045; (*c*) Y. Liu and S. S. Feng, *J. Controlled Release*, 2011, **152**, e64–e65; (*d*) Z. Zhang and S. S. Feng, *Biomaterials*, 2006, **27**, 262–270; (*e*) P. Howes, M. Green, J. Levitt, K. Suhling and M. Hughes, *J. Am. Chem. Soc.*, 2010, **132**, 3989–3996; (*f*) Z. M. Tao, G. S. Hong, C. Shinji, C. X. Chen, S. Diao, A. L. Antaris, B. Zhang, Y. P. Zou and H. J. Dai, *Angew. Chem., Int. Ed.*, 2013, **52**, 13002–13006; (*g*) I. Ozcan, K. Bouchemal, F. Segura-Sanchez, O. Ozer, T. Guneri and G. Ponchel, *J. Pharm. Sci.*, 2011, **100**, 4877–4887.

6 (*a*) D. Ding, J. Liu, G. Feng, K. Li, Y. Hu and B. Liu, *Small*, 2013, **9**, 3093–3102; (*b*) C. Kim, C. Favazza and L. V. Wang, *Chem. Rev.*, 2010, **110**, 2756–2782.

7 (*a*) P. Wu, S. Kuo, Y. Huang, C. Chen and Y. Chan, *Anal. Chem.*, 2014, **86**, 4831–4839; (*b*) Y. Jin, F. Ye, M. Zeigler, C. Wu and D. Wu, *ACS Nano*, 2011, **5**, 1468–1475.

8 (*a*) W. Zhang, H. Sun, S. Yin, J. Chang, Y. Li, X. Guo and Z. Yuan, *J. Mater. Sci.*, 2015, **50**, 5571–5577; (*b*) J. O. Escobedo, O. Rusin, S. Lim and R. M. Strongin, *Curr. Opin. Chem. Biol.*, 2010, **14**, 64–70.

9 (*a*) M. B. Zeigler, W. Sun, Y. Rong and D. T. Chiu, *J. Am. Chem. Soc.*, 2013, **135**, 11453–11455; (*b*) B. Liu and G. C. Bazan, *Chem. Mater.*, 2004, **16**, 4467–4476; (*c*) K. Y. Pu and B. Liu, *Adv. Funct. Mater.*, 2011, **21**, 3408–3423; (*d*) A. Duarte, K. Y. Pu, B. Liu and G. C. Bazan, *Chem. Mater.*, 2011, **23**, 501–505; (*e*) L. Feng, C. Zhu, H. Yuan, L. Liu, F. Lv and S. Wang, *Chem. Soc. Rev.*, 2013, **42**, 6620–6633; (*f*) K. Li and B. Liu, *J. Mater. Chem.*, 2012, **22**, 1257–1264.

10 J. Liu, G. Feng, D. Ding and B. Liu, *Polym. Chem.*, 2013, **4**, 4326–4334.

11 (*a*) C. Chen, Y. Huang, S. Liou, P. Wu, S. Kuo and Y. Chan, *ACS Appl. Mater. Interfaces*, 2014, **6**, 21585–21595; (*b*) C. Wu, B. Bull, C. Szymanski, K. Christensen and J. McNeill, *ACS Nano*, 2008, **2**, 2415–2423; (*c*) C. F. Wu, S. J. Hansen, Q. O. Hou, J. B. Yu, M. Zeigler, Y. H. Jin, D. R. Burnham, J. D. McNeill, J. M. Olson and D. T. Chiu, *Angew. Chem., Int. Ed.*, 2011, **50**, 3430–3434.

12 (*a*) J. Song, Y. Guo, L. Liu and H. Wang, *Dyes Pigm.*, 2015, **122**, 184–191; (*b*) Y. Zhou, M. Li, Y. Guo, H. Lu, J. Song, Z. Bo and H. Wang, *ACS Appl. Mater. Interfaces*, 2016, **8**, 31348–31358.